

LAVAL-PHY-96-17
ALBERTA-THY-39-96

Scalar Leptoquark Pair Production at the CERN LHC: Signal and Backgrounds

B. Dion, L. Marleau, G. Simon

*Département de Physique, Université Laval
Québec QC Canada, G1K 7P4*

M. de Montigny

*Faculté Saint-Jean, University of Alberta
Edmonton AB Canada, T6C 4G9
(1996)*

Abstract

We present the results of an analysis for the pair production of scalar leptoquarks at the CERN Large Hadron Collider (LHC) with $\sqrt{s} = 14$ TeV and $\mathcal{L} = 10 \text{ fb}^{-1}$ which includes the dominant sources of Standard Model background associated to this process: $Z^* jj$ and $t\bar{t}$ production. We consider leptoquarks introduced in the framework of a supersymmetric grand unified E_6 model. The leptoquark production is found to be dominant in most regions of parameter space, except near the Z pole where the Drell-Yan background is peaked. Otherwise the $t\bar{t}$ process provides the main source of background. We establish the discovery reach of the leptoquarks at 750 GeV (1 TeV) for a branching ratio of $BR(LQ \rightarrow eq) = 0.5$ ($BR = 1$).

PACS numbers: 11.25.Mj, 13.85.Qk, 14.80.-j.

Typeset using REVTeX

I. INTRODUCTION

A particular challenge of the future colliders—such as the proton-proton LHC (CERN)—will be to unravel the existence of exotic phenomena, which would manifest themselves through new interactions of standard particles or through the production of new particles. Here we are interested in the latter type of manifestation of physics beyond the Standard Model (SM): we investigate the pair production of scalar leptoquarks. Leptoquarks occur in various extensions of the SM, such as composite [1], GUT [2] and SUSY [3] models, as exotic particles which carry both color and lepton quantum numbers. In general they are spin 0 or 1 bosons, with mass and coupling constant to the standard fermions left as unknown parameters. However, experimental constraints have been set on these parameters quite recently [4,5,6].

The leptoquark pair production at hadron colliders has a clear advantage over any other method of detection: it is almost insensitive to the magnitude of the Yukawa coupling. Previous searches performed at the proton-antiproton collider Tevatron (Fermilab) have excluded leptoquarks with masses below 133 GeV and 120 GeV for branching ratios of the leptoquarks to the electron equal to 1 and 0.5, respectively, and somewhat lower limits for the branching to muons [4]. Similar searches have also been performed at LEP [5] and HERA [6]. A large machine like the LHC (with $\sqrt{s} = 14$ TeV and $\mathcal{L} = 10 \text{ fb}^{-1}$) should improve considerably such discovery limits.

The cross sections for the pair production of scalar leptoquarks at hadron colliders can be found in the literature [7,8]. However, a comprehensive study of the various QCD and electroweak backgrounds which accompany leptoquark processes has been lacking up until recently [9]. Indeed, it is not trivial otherwise to estimate to which extent the leptoquark signal will “survive” the QCD production of heavy fermions, or jets produced along with the vector bosons W and Z , etc. Here, we shall consider events where both leptoquarks decay into an electron plus quark, implying a 2 jets + e^+e^- signature.

The purpose of this paper is to investigate the ability of the CERN Large Hadron Collider (by using the design of the ATLAS and CMS experiments [10,11]) to unravel the presence of scalar leptoquarks and to examine to which extent the leptoquark signal can be distinguished from Standard Model processes. We implement leptoquark data and related cross sections in the ISAJET event generator and use the ISZRUN package contained in the Zebra version to perform our selection cuts.

We consider the scalar leptoquarks contained in the supersymmetric grand unified E_6 model (the low-energy limit of an $E_8 \otimes E_8$ heterotic string theory [12]). In the E_6 model, each matter supermultiplet lies in the fundamental **27** representation, which contains, in addition to the usual quarks and leptons (and their superpartners), new particles such as two fiveplets (D, H) and (\bar{D}, \bar{H}) and an $SU(5)$ superfield singlet N . We focus on the superfields D and \bar{D} which are two $SU(3)$ triplets and $SU(2)$ singlets with electromagnetic charges $-1/3$ and $+1/3$, respectively. Depending on the charge assignment chosen for the superfields, D and \bar{D} can be taken to possess $B = \pm 1/3$ and $L = \pm 1$. The scalar superpartners of these superfields are the object of the present study. We thus consider scalar leptoquarks with $Q = -1/3$. We restrict our study to the first generation of fermions. The Yukawa interactions take the form:

$$\mathcal{L}_Y = \lambda_L \tilde{D}^{c*} (e_L u_L + \nu_L d_L) + \lambda_R \tilde{D} e_L^c u_L^c + \text{h.c.} \quad (1)$$

where c denotes the charge conjugate state, and \tilde{D} is the scalar superpartner of D . In this model, the λ are independent and arbitrary but we choose them to be equal to the electromagnetic charge, following [13]. It is important to note that leptoquarks also interact strongly. As we shall see, these interactions are mainly responsible for their pair production.

In the following Section, we present the details of our simulation and the selection cuts that we have chosen. Next, we elaborate on the expected signature of the leptoquark signal and of the principal sources of background: Drell-Yan and $t\bar{t}$ production. Finally, we summarize our results and conclude in Section 5.

II. EVENT SIMULATION

A. Detector and calorimeter

We use the toy calorimeter simulation package ISZRUN contained in the Zebra version of ISAJET [14] to simulate the experimental conditions at the LHC, with the ATLAS and CMS detectors in mind:

- cell size: $\Delta\eta \times \Delta\phi = 0.05 \times 0.05$,
- pseudorapidity range: $-5 < \eta < 5$,
- hadronic energy resolution: $50\%/\sqrt{E} \oplus 0.03$ for $-3 < \eta < 3$,
 $100\%/\sqrt{E} \oplus 0.07$ for $3 < |\eta| < 5$,
- electromagnetic energy resolution: $10\%/\sqrt{E} \oplus 0.01$.

B. Kinematic cuts

For the purposes of this work, hadronic showers are regarded as jets when they lie within a cone of radius

$$R = \sqrt{(\Delta\eta)^2 + (\Delta\phi)^2} = 0.7,$$

possess a transverse energy

$$E_T > 25 \text{ GeV},$$

and a pseudorapidity

$$|\eta_j| \leq 3.$$

Similarly, electrons are considered isolated if they are separated from any jet by

$$R \geq 0.3,$$

have a transverse momentum

$$p_T > 75 \text{ GeV},$$

and a pseudorapidity

$$|\eta_l| \leq 2.5.$$

Our calculations are performed using the PDFLIB distribution functions of Morfin and Tung (M-T B2) with $\Lambda = 191$ GeV [15,16].

III. LEPTOQUARK SIGNAL AND BACKGROUNDS

Here, we consider first-generation leptoquarks, which can decay into either an u -quark and an electron, or into a d -quark and a ν_e . For the purposes of our calculations, we consider the case in which both occur with equal probability ($BR = 0.5$). We also assume a Yukawa coupling of electromagnetic strength $\alpha_Y = \alpha_{em}$ (in fact, it is a generic feature of string-inspired models that the non-zero Yukawa coupling is of the same order as the gauge coupling [17]). In fact, the Yukawa coupling has only a very small impact on the pair production cross section.

A. Leptoquark signal

We analyze the pair production of scalar leptoquarks which arise from two subprocesses: (1) quark-antiquark annihilation ($u_R + u_L^c \rightarrow \tilde{D} + \tilde{D}^*$ and $u_L + u_R^c \rightarrow \tilde{D}^{c*} + \tilde{D}^c$), and (2) gluon fusion ($g + g \rightarrow \tilde{D} + \tilde{D}^*$ and $g + g \rightarrow \tilde{D}^{c*} + \tilde{D}^c$) (see Fig. 1). Whereas the first subprocess occurs in the s -channel (through the exchange of a virtual gluon) and in the t -channel (virtual electron), subprocess (2) arises via color gauge interactions from the trilinear term gDD in the s -channel (through the exchange of a gluon) and in the t - and u -channels (exchange of virtual scalar leptoquarks), and from the quartic term $ggDD$ in which two gluons annihilate to produce a pair of leptoquarks. We expect the gluon fusion channel to dominate at the LHC.

Leptoquark pair production can lead to three distinct signals:

- (a) 2 jets + e^+e^- ,
- (b) 2 jets + \not{p}_T ,
- (c) 2 jets + $e^\pm + \not{p}_T$.

The most striking of these signals is expected to be (a). In fact, signals (b) and (c) are more cumbersome because many SM (WW , WZ , ZZ , Zgg and Zgq production) and SUSY processes have the same signatures. We therefore restrict ourselves to 2 jets + e^+e^- . The background, which comes from Z^*jj and $t\bar{t}$ can be considerably reduced by requiring a cut on the transverse energy of the jets and leptons. Here we shall impose the same E_T cut on the leptons and the jets.

B. SM Backgrounds

The most probable sources of background as identified by Refs. [7] are (1) Z^*jj , (2) $t\bar{t}$, (3) ZZ and WZ production. However, our early calculations have shown processes (3) to be negligible compared to the other two (see also [9]). Therefore, we will restrict ourselves to processes (1) and (2). Some examples these processes are shown in Fig. 2.

1. Z^*jj background

The Z^*jj background occurs when a Drell-Yan virtual Z (producing a pair of leptons) is accompanied by the production of two jets: $pp \rightarrow Z^*jj \rightarrow e^+e^-jj$ where $j = q, \bar{q}, g$. A previous study for the Tevatron [9] has shown this process to be important near the Z pole but small otherwise. We consider this background for an invariant mass of the lepton pair ranging from 100 GeV to 1 TeV.

2. $t\bar{t}$ background

The other source of background we consider comes from $t\bar{t}$ where the top is decaying into a b quark, an electron and a ν_e . The presence of neutrinos implies in general a missing transverse momentum \not{p}_T . In this case, it is natural to expect the available transverse energy of the electron to be smaller on average than that involved in the leptoquark process. However, we have found previously at the Tevatron [9] that $t\bar{t}$ production provides the main source of background at masses above the Z peak. Our calculations were made using $M_t=175$ GeV.

IV. LEPTOQUARK DISCOVERY REACH AT THE CERN LHC

Figures 3-6 show the total cross section for 2 jets + e^+e^- as a function of the mass without cuts on \not{p}_T , for transverse energies E_T larger than 50, 100, 150 and 200 GeV respectively. The leptoquark signal (solid lines) is plotted against the invariant mass of the lepton-quark pair whereas the Z^*jj (dot-dashed lines) is plotted against the invariant mass of the lepton pair. The $t\bar{t}$ background (dashed lines) is evaluated at $M_t=175$ GeV.

Figures 7-8 exhibit the same physical quantities as Figs. 4 and 6 except that we impose an additional cut on missing transverse momentum of $\not{p}_T < 100$ GeV and $\not{p}_T < 200$ GeV respectively. The contributions from the production of leptoquarks, $t\bar{t}$, and Z^*jj are explicitly illustrated with the same conventions. These figures show a Z^*jj background peaked at small masses and E_T cut. This is essentially due to the Z pole. This background could be suppressed by imposing a cut on the invariant mass of the lepton pair but it turns out that an E_T cut larger than 150 GeV is sufficient here.

The second source of background comes from $t\bar{t}$ production which overwhelms the leptoquark signal for an E_T cut of 50 GeV (Fig.3). For an E_T cut of 100 (150) GeV, the leptoquark signal is dominant for $M_{LQ} < 450$ (700) GeV (Figs.4-5). Moreover, Figs. 3 and 6 show that the increase of the E_T cut from 50 GeV to 200 GeV brings down the $t\bar{t}$ background by almost one order of magnitude while leaving the leptoquark signal unaffected.

Figures 9 and 10 show the total production cross section in terms of the E_T cut for leptoquark masses equal to 250 (solid lines), 500 (dashed), 750 (dot-dashed) and 1000 (dotted) GeV and for $M_t=175$ GeV (dot-dot-dashed lines). These figures illustrate more clearly the overall effect of the E_T cut. For instance, the leptoquark signal is optimized when the E_T cut is between 100 and 200 GeV. When smaller E_T cuts are used, the number of jets in a given event can easily grow to 3 or 4 and the event is eventually discarded. We can also see from Figs. 9 and 10 that the $t\bar{t}$ background exhibits a smooth logarithmic behavior.

A detailed analysis showed that the $t\bar{t}$ background is not affected by the E_T cut on the hadronic jets. On the other hand, it turns out to be more sensitive to an E_T cut on the electrons. This is due to the fact that the neutrinos will in general escape with a large fraction of the available transverse energy. If we compare Fig. 4 with Fig. 7 and Fig. 6 with Fig. 8, we see that the overall effect of the missing \not{p}_T cut is to increase the signal-to-background ratio. The leptoquark signal is practically unaffected by the cut while the $t\bar{t}$ production is reduced by almost one order of magnitude.

We require 10 events and a background suppressed by 5σ for leptoquark discovery. Assuming a luminosity of 10 fb^{-1} , this implies that a leptoquark is observable if its production cross section is larger than 1 fb while the background does not exceed 0.4 fb . From our calculations, we found that the optimal cuts are $E_T > 200 \text{ GeV}$ and $\not{p}_T < 200 \text{ GeV}$ (see Fig. 8). Using these constraints, we find a discovery reach of 750 GeV for leptoquarks that decay into electrons with $BR = 0.5$. We can also evaluate the discovery reach for leptoquarks that decay with $BR = 1$ recalling that the cross section for the production of 2 jets $+ e^+e^-$ is four times larger in this case. We can thus estimate the discovery reach to 1 TeV for leptoquarks that decay to electrons with $BR = 1$. Our discovery limits are somewhat lower than those recently obtained in Ref. [18]. This is expected since the cuts that we have applied to suppress the background have also reduced the signal cross section.

V. CONCLUSION

To summarize, we have presented the results of an analysis of the first-generation scalar leptoquark pair production within the context of an E_6 model. We have also calculated the importance of the various Standard Model backgrounds which could potentially have the same signature. The leptoquark signal was found to be dominant over the Z^*jj background except near the Z pole. In the case of the $t\bar{t}$ background, we obtain a satisfactory signal-to-background ratio for values of E_T at or above 200 GeV but we evaluated our discovery limit for the optimal case: $E_T > 200 \text{ GeV}$ and $\not{p}_T < 200 \text{ GeV}$. We found a leptoquark discovery reach of 750 GeV (1 TeV) for a branching ratio of $BR(LQ \rightarrow eq) = 0.5$ ($BR = 1$).

ACKNOWLEDGMENTS

We are indebted to Pr. J. Pinfold for useful comments. The authors would like to thank Pr. Frank Paige for answering numerous questions during the installation of ISAJET and P. Spiers for his help during the calculations. This research was supported by the Central Research Fund of the University of Alberta, contract no CRF-GEN 81-53428, the Natural

Sciences and Engineering Research Council of Canada, and by the Fonds pour la Formation de Chercheurs et l'Aide à la Recherche du Québec.

REFERENCES

- [1] L. Abbott and E. Fahri, Phys. Lett. **B101**, 69 (1981); Nucl. Phys. **B189**, 547 (1981); B. Schrempp and F. Schrempp, Phys. Lett. **B153**, 101 (1985) and references therein; J. Wudka, Phys. Lett. **B167**, 337 (1986).
- [2] H. Georgi and S. L. Glashow, Phys. Rev. Lett. **32**, 438 (1974); J. C. Pati and A. Salam, Phys. Rev. **D10**, 275 (1974); Phys. Rev. Lett. **31**, 661 (1975); S. Dimopoulos and L. Susskind, Nucl. Phys. **B155**, 237 (1979); S. Dimopoulos, Nucl. Phys. **B168**, 69 (1980) P. Langacker, Phys. Rep. **72**, 185 (1981); G. Senjanović and A. Šoborac, Z. Phys. **C20**, 255 (1983); R. J. Cashmore *et al.*, Phys. Rep. **122**, 275 (1985).
- [3] E. Eichten *et al.*, Phys. Rev. Lett. **50**, 811 (1983); J. L. Hewett and T. G. Rizzo, Phys. Rep. **183**, 193 (1989); S. Dimopoulos, Nucl. Phys. **B168**, 69 (1981); E. Farhi and L. Susskind, Phys. Rev. **D20**, 3404 (1979); Phys. Rep. **74**, 277 (1981); V. D. Angelopoulos *et al.*, Nucl. Phys. **B292**, 59 (1987); J. F. Gunion and E. Ma, Phys. Lett. **B195**, 257 (1987); R. W. Robinett, Phys. Rev. **D37**, 1321 (1988); J. A. Grifols and S. Peris, Phys. Lett. **B201**, 287 (1988).
- [4] S. Abachi *et al.* (D0 Collaboration), Phys. Rev. Lett. **72**, 965 (1994); **75**, 3618 (1995); F. Abe *et al.* (CDF Collaboration), Phys. Rev. **D48**, R3939 (1993); Phys. Rev. Lett. **75**, 1012 (1995); J. Alitti *et al.* (UA2 Collaboration), Phys. Lett. **B274**, 507 (1992).
- [5] G. Alexander *et al.* (OPAL Collaboration), Phys. Lett. **B275**, 123 (1992); Phys. Lett. **B263**, 123 (1991); D. Decamp *et al.* (ALEPH Collaboration), Phys. Rep. **216**, 253 (1992); B. Adeva *et al.* (L3 Collaboration), Phys. Lett. **B261**, 169 (1991); O. Adriani *et al.* (L3 Collaboration), Phys. Rep. **236**, 1 (1993); P. Abreu *et al.* (DELPHI Collaboration), Phys. Lett. **B275**, 222 (1992); **B316**, 620 (1993).
- [6] I. Abt *et al.* (H1 Collaboration), Nucl. Phys. **B396**, 3 (1993); M. Derrick *et al.* (ZEUS Collaboration), Phys. Lett. **B306**, 173 (1993); T. Ahmed *et al.* (H1 Collaboration), Z. Phys. **C64**, 545 (1994); S. Aid *et al.* (H1 Collaboration), Phys. Lett. **B353**, 578 (1995); **B369**, 173 (1996).
- [7] J. L. Hewett and S. Pakvasa, Phys. Rev. **D37**, 3165 (1988); O.J.P. Éboli and A.V. Olinto, Phys. Rev. **D38**, 3461 (1988).
- [8] M. de Montigny, L. Marleau and G. Simon, Phys. Rev. **D52**, 533 (1995); M. de Montigny and L. Marleau, Phys. Rev. **D40**, 2869 (1989); Can. J. Phys. **68**, 612 (1990)
- [9] B. Dion, L. Marleau and G. Simon, LAVAL-PHY-96-16 and hep-ph/9610397.
- [10] W.W. Armstrong *et al.*, *ATLAS Technical Proposal*, CERN/LHCC/94-43 (1994).
- [11] G.L. Bayatian *et al.*, *CMS Technical Proposal*, CERN/LHCC/94-38 (1994).
- [12] M. Green and J. Schwarz, Phys. Lett. **B149**, 117 (1984); E. Witten, Nucl. Phys. **B258**, 75 (1985); D. Gross, J. Harvey, E. Martinec and R. Rohm, Phys. Rev. Lett. **54**, 502 (1985); Nucl. Phys. **B256**, 253 (1985); **B267**, 75 (1986); M. B. Green, J. H. Schwarz and E. Witten, “Superstring Theory”, Cambridge University Press, New York (1987).
- [13] J. L. Hewett and T. G. Rizzo, Phys. Rev. **D36**, 3367, (1987).
- [14] F. Paige and S. Protopopescu, “Supercollider Physics”, World Scientific (1986); H. Baer, F. Paige, S. Protopopescu and X. Tata, “Proceedings of the Workshop on Physics at Current Accelerators and Supercolliders”, Argonne National Laboratory (1993).
- [15] J. G. Morfin and W. K. Tung, Z. Phys. **C52**, 13 (1991).
- [16] H. Plothow-Besh, Comput. Phys. Commun. **75**, 396 (1993).
- [17] E. Witten, Phys. Lett. **B155**, 151 (1985).

[18] J. Blümlein, E. Boos and A. Kryukov, DESY 96-174 and hep-ph/ 9610408.

FIGURES

FIG. 1. Feynman diagrams for leptoquark pair production via ((a), (b)) $q\bar{q}$ annihilation and ((c), (d), (e), (f)) gluon fusion.

FIG. 2. Examples of Feynman diagrams for (a) Z^*jj and (b) $t\bar{t}$ production.

FIG. 3. Cross section for the production of 2 jets + e^+e^- as a function of the relevant invariant mass for $E_T > 50$ GeV. The full line corresponds to the leptoquark signal versus the leptoquark mass (M_{LQ}), the dash-dotted line to Z^*jj signal versus the e^+e^- invariant mass ($M_{e^+e^-}$) and the dashed line to $t\bar{t}$ background for $M_t = 175$ GeV.

FIG. 4. Same as figure 3 but for $E_T > 100$ GeV.

FIG. 5. Same as figure 3 but for $E_T > 150$ GeV.

FIG. 6. Same as figure 3 but for $E_T > 200$ GeV.

FIG. 7. Same as figure 3 but for $E_T > 100$ GeV and $\not{p}_T < 100$ GeV.

FIG. 8. Same as figure 3 but for $E_T > 200$ GeV and $\not{p}_T < 200$ GeV.

FIG. 9. Cross section for the production of 2 jets + e^+e^- as a function of E_T for $M_{LQ} = 250$ (solid line), 500 (dashed), 750 (dot-dashed) and 1000 (dotted) GeV. The dot-dot-dashed line corresponds to $t\bar{t}$ production for $M_t = 175$ GeV.

FIG. 10. Same as figure 9 with an additional cut on \not{p}_T .

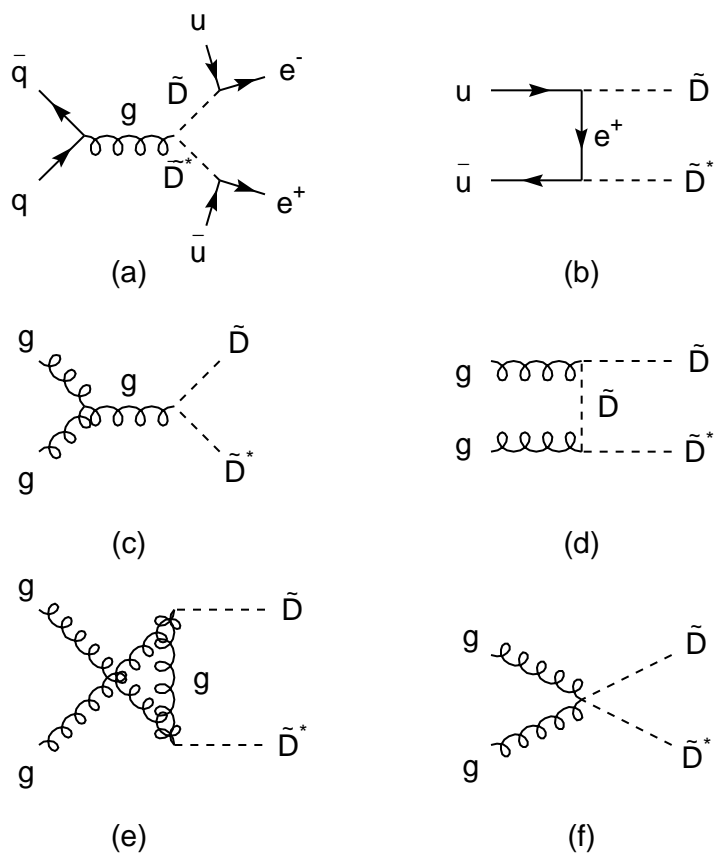


Figure 1

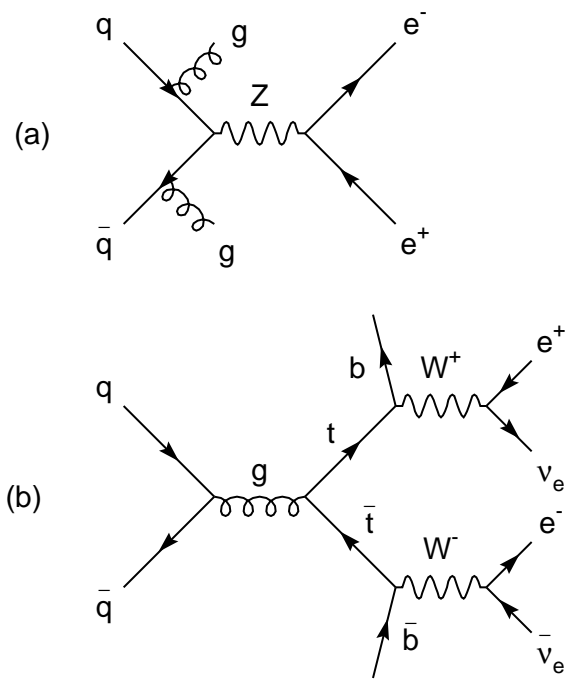


Figure 2

Figure 3

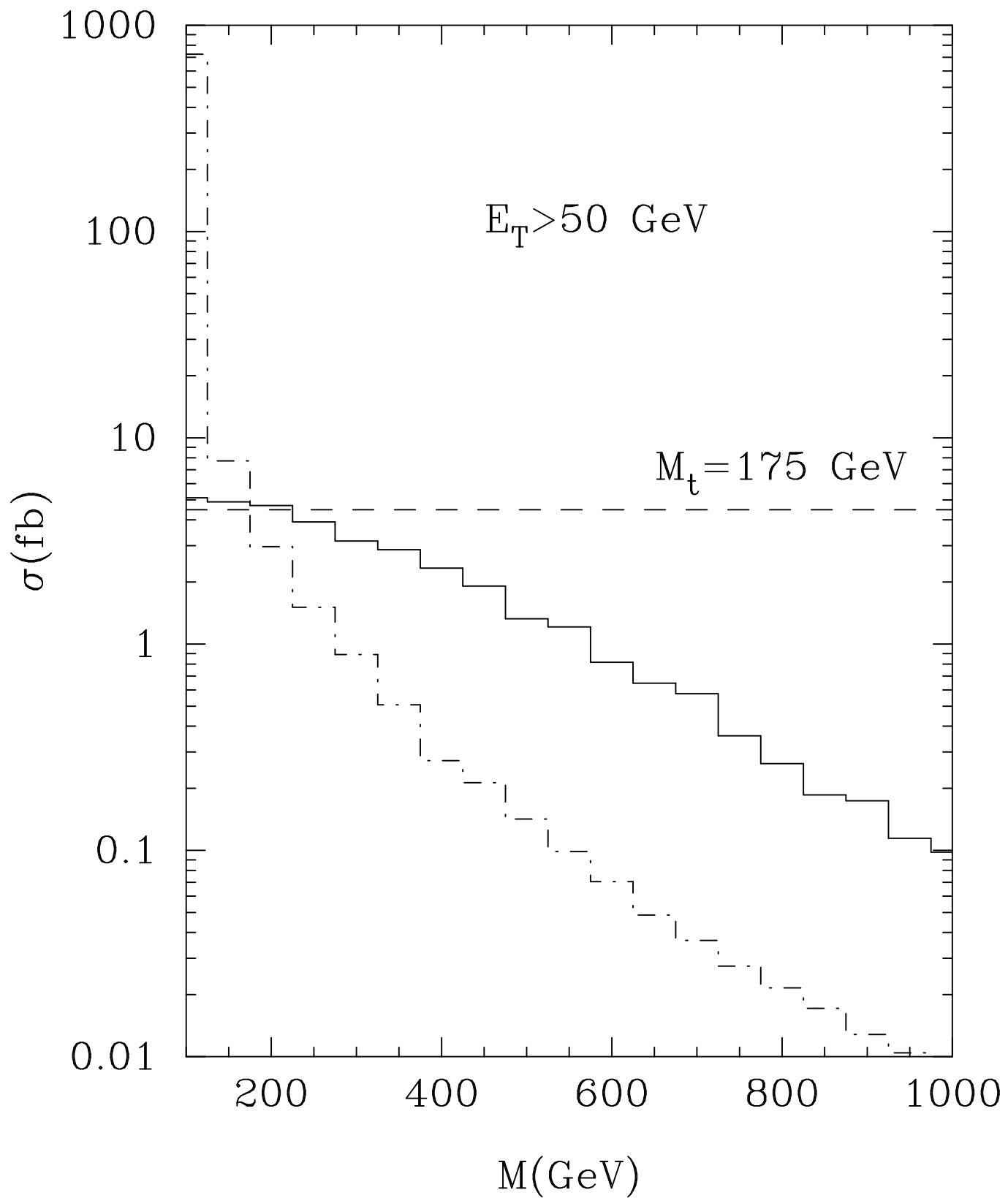


Figure 4

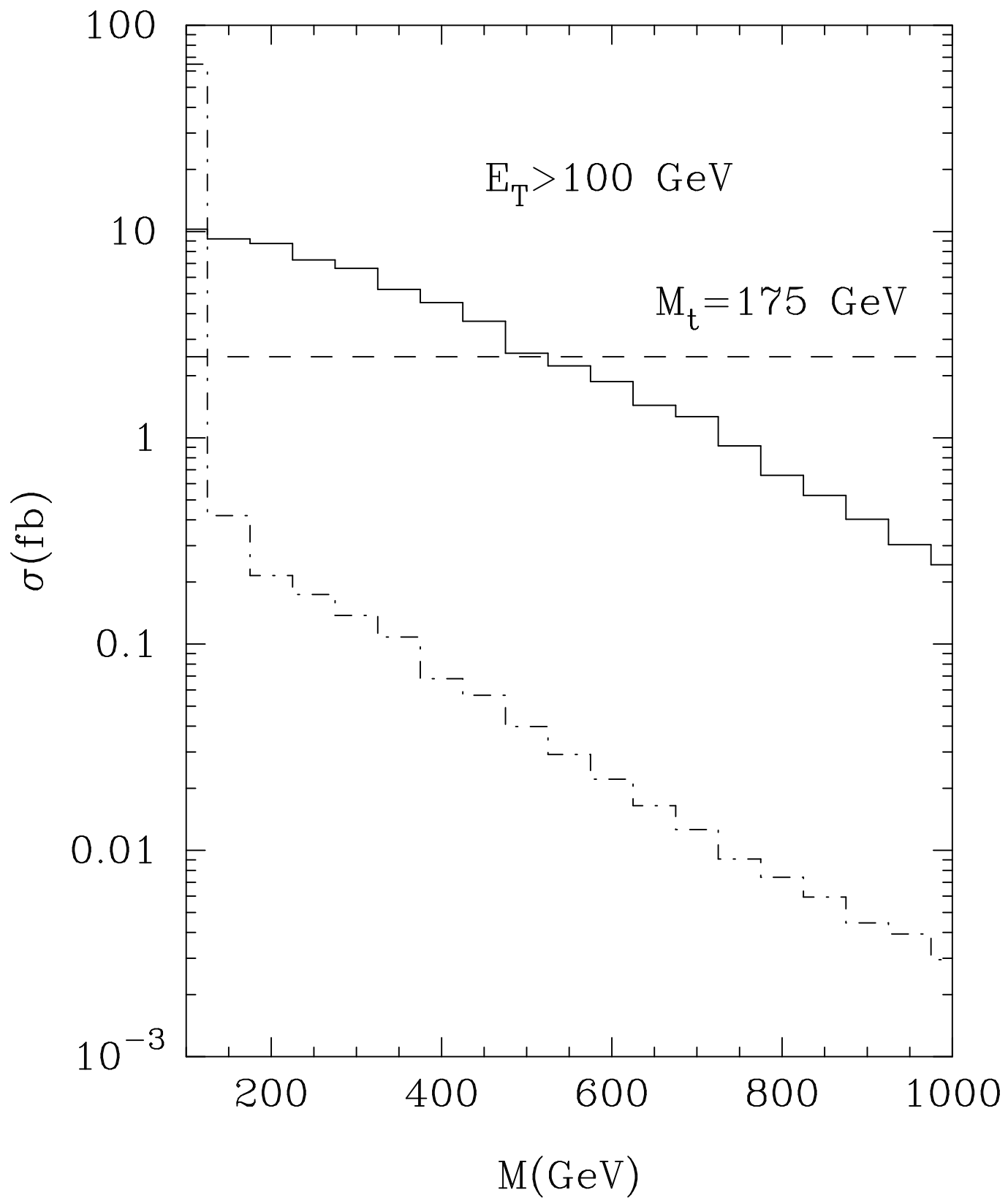


Figure 5

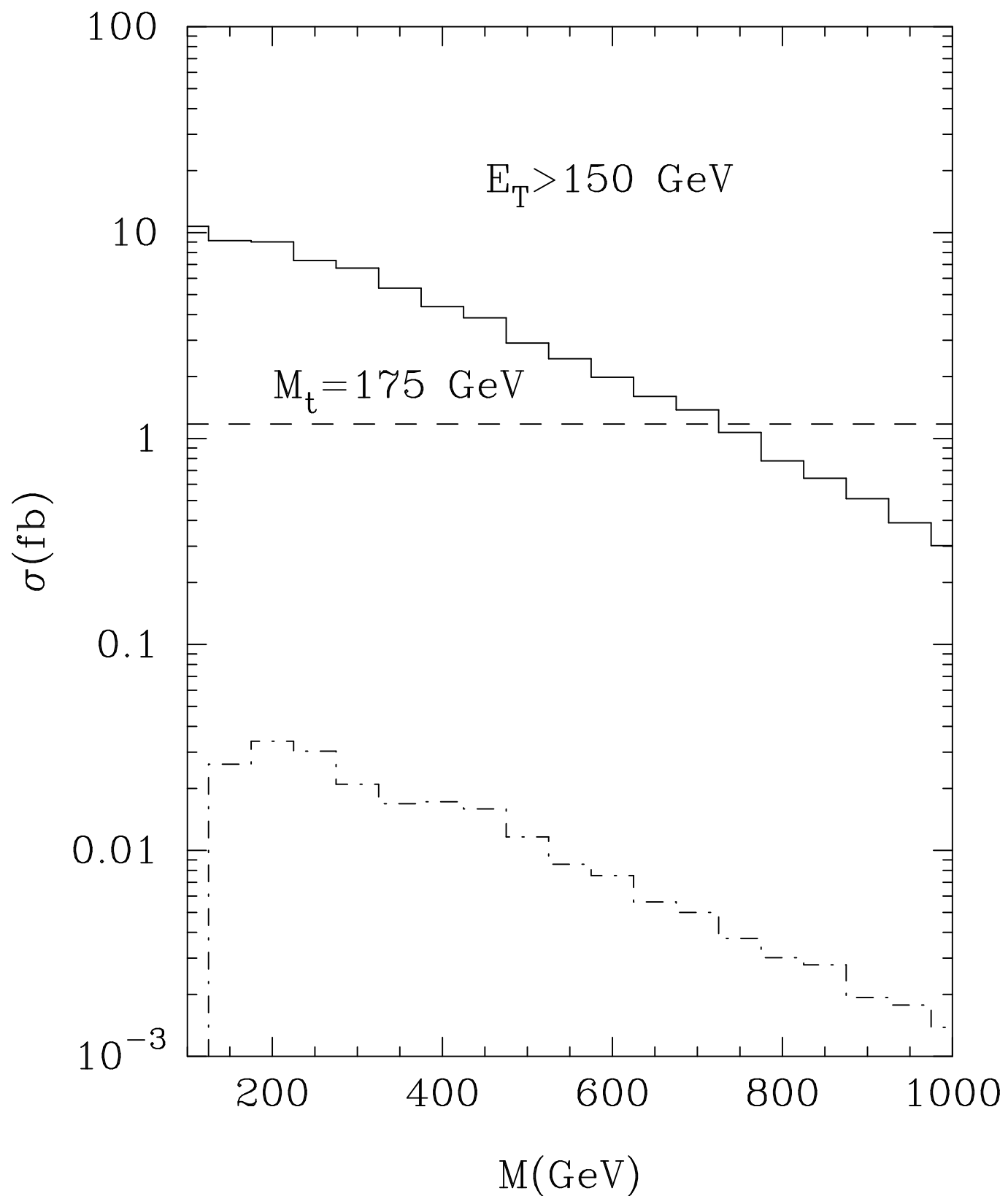


Figure 6

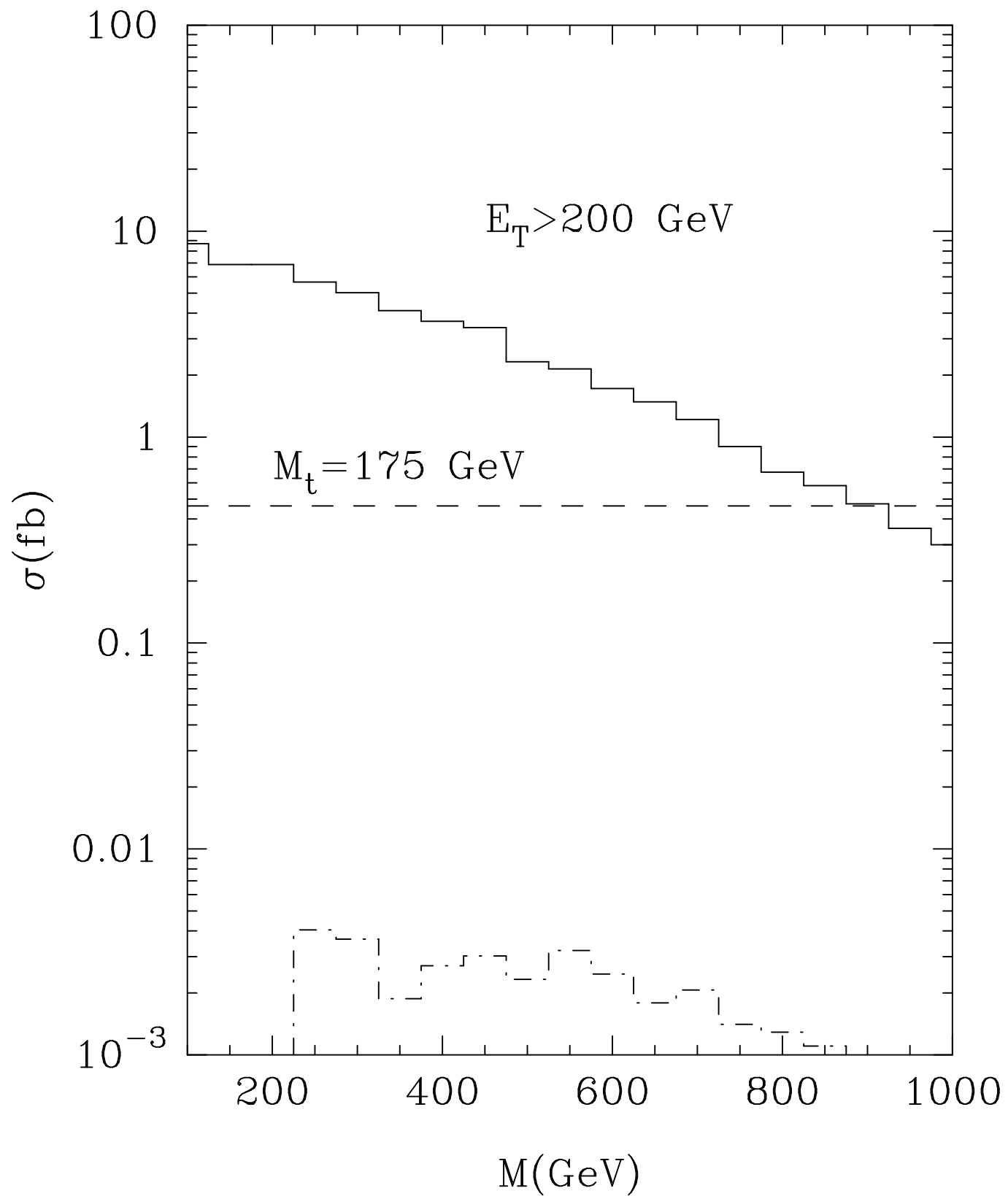


Figure 7

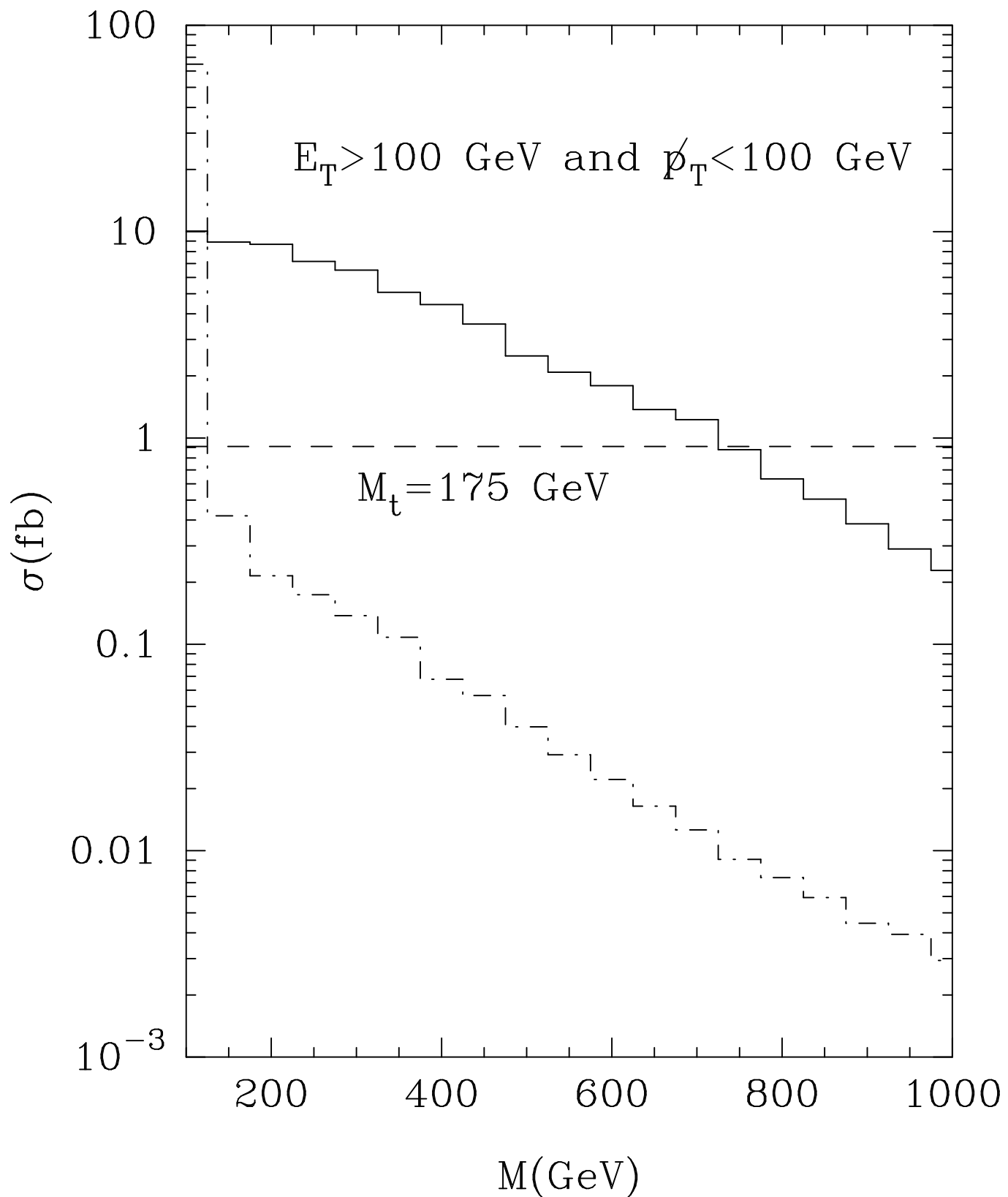


Figure 8

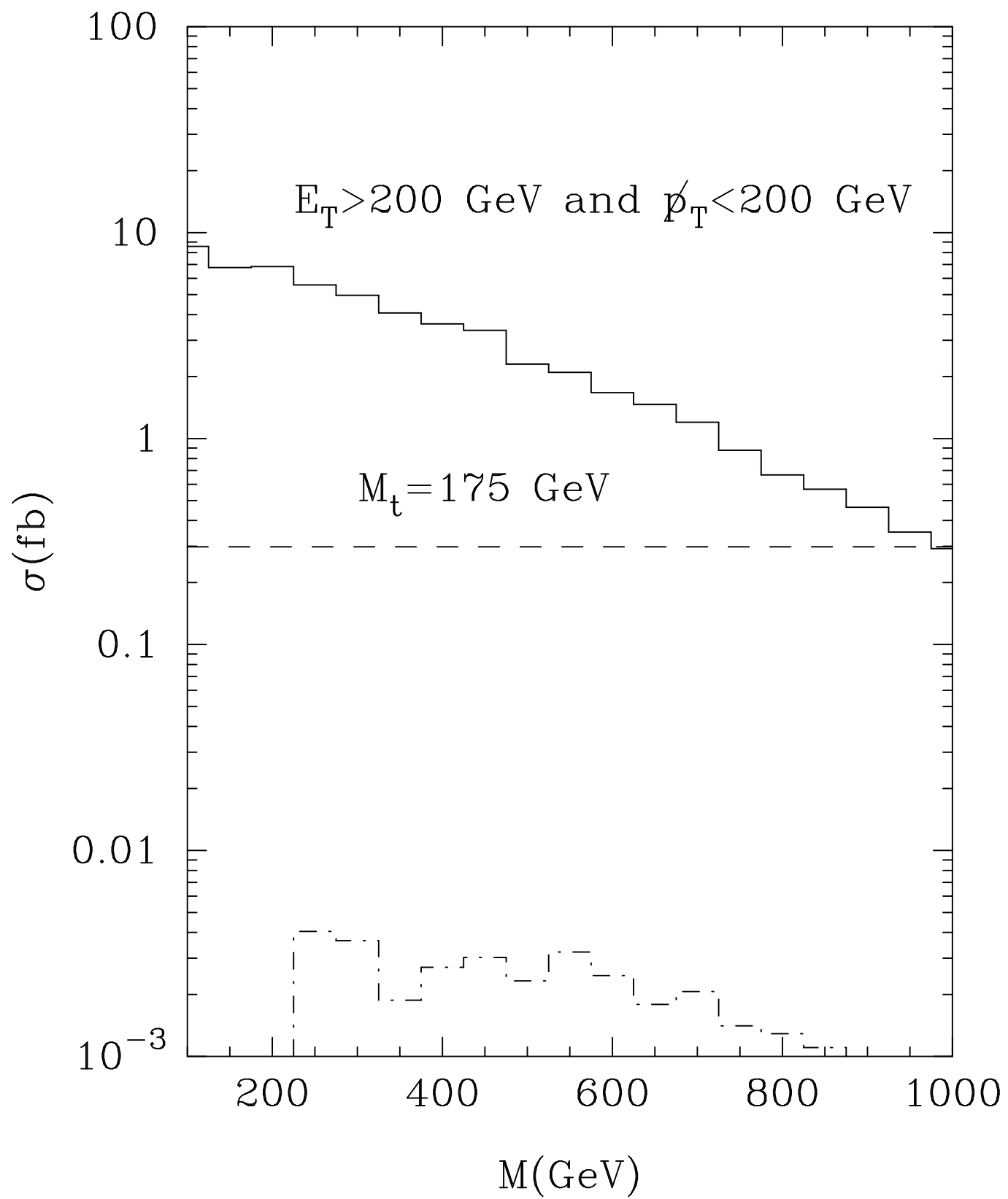


Figure 9

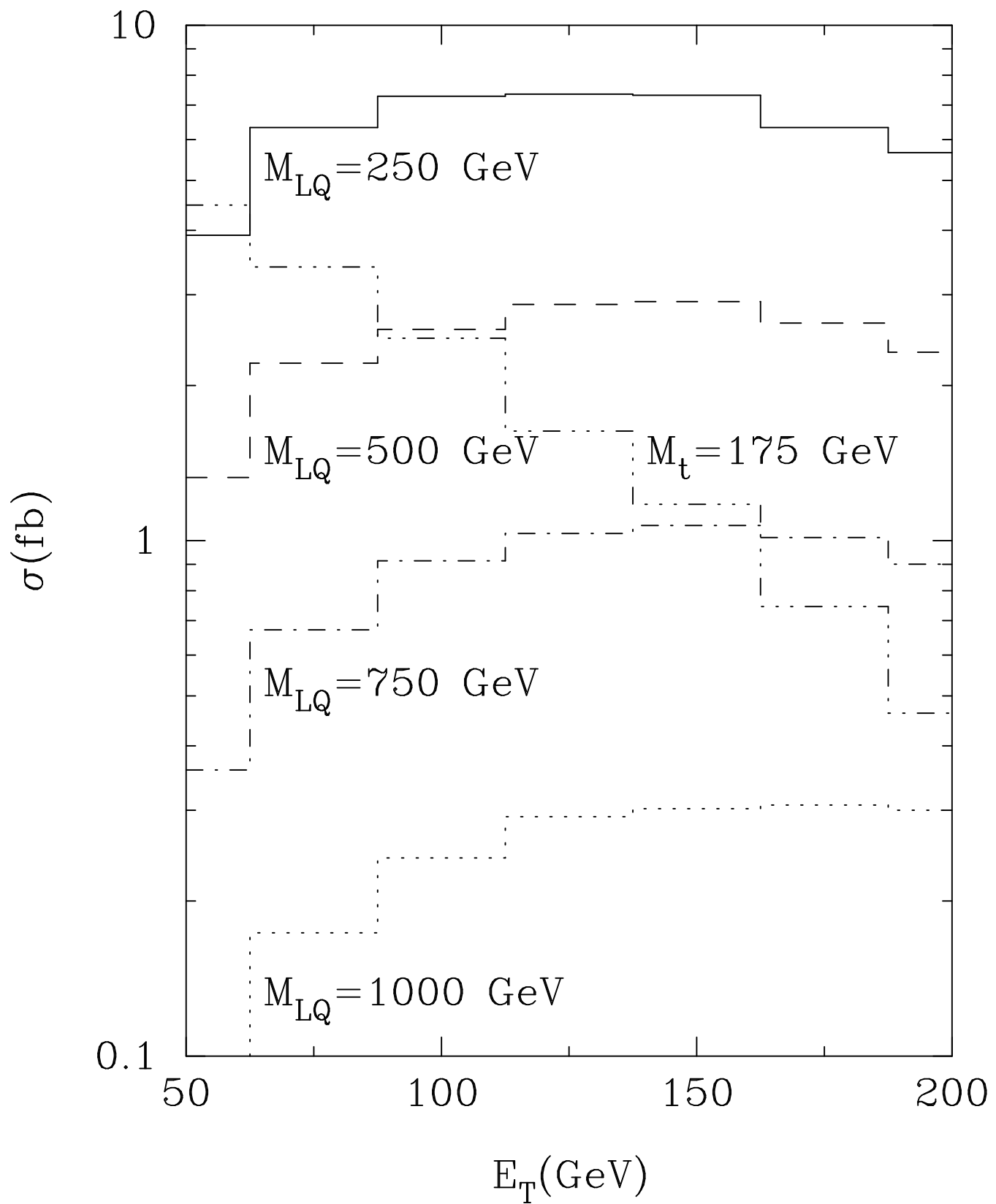


Figure 10

